Supporting Information for

Halogen radicals contribute to photo-oxidation in coastal and estuarine waters

Kimberly M. Parker,[a] *William A. Mitch*[a,1]

[a]Department of Civil and Environmental Engineering, Stanford University, 473 Via Ortega, Stanford, California 94305, USA

[1]CORRESPONDING AUTHOR

Email: wamitch@stanford.edu

Supporting Information Contents

Results

Contribution of photochemical pathways in DOM-sensitized matrices. The overall domoic acid photodegradation in the synthetic matrices was attributed to corresponding photochemical pathways using a series of experiments designed to isolate, promote or quench specific reaction pathways. The experimental data (presented in Table S1) was used to develop the results presented in Figure 1c.

Direct photolysis. To quantify the contribution of direct photolysis to domoic acid degradation in the synthetic matrices, domoic acid loss was measured in DI water containing 20 mM phosphate buffer (pH 8.1) alone (freshwater), with 540 mM $NaClO_4$ (ionic strength control), and 540 mM NaCl, 0.8 mM NaBr (seawater halides). The observed rate constants are reported in Table S1. To calculate the contribution of direct photolysis to total domoic acid photodegradation in the presence of sensitizers, the rate constants were corrected for shading (1) occurring due the presence of 5 mg/L DOM as Suwannee River DOM (SRDOM).

Overall, direct photolysis accounted for 23% (freshwater), 21% (ionic strength control), and 14% (seawater halides) of the photodegradation observed in the presence of 5 mg/L SRDOM. Some matrix effect was observed, suggesting that self-sensitization may be occurring. However, because domoic acid concentrations were the same in the direct and SRDOM-containing experiments, the same extent of self-sensitization is expected to occur in both sets of matrices.

Indirect photolysis. The indirect photodegradation rate constant in the SRNOM-containing synthetic solutions was calculated by subtracting the shading-corrected direct rate constant from the total observed rate constant in the presence of 5 mg-C/L SRNOM. In this way, the indirect photolysis rate constants were determined to be 5.5 (±0.3)× 10^{-6} s^{-1} in freshwater, 8.7 (±0.4)× 10^{-6} s^{-1} in the ionic strength control and 21.8 (±1.1)× 10^{-6} s^{-1} in the presence of seawater halides. Therefore, the presence of seawater-level ionic strength increased the indirect photodegradation rate constant of domoic acid by 3.2 (±0.5)× 10^{-6} s^{-1}, and the presence of seawater halides specifically increased the indirect photodegradation rate constant of domoic acid by 13.1 (±1.2)× 10^{-6} s^{-1}.

Singlet oxygen. One reactive oxygen species (ROS) that could contribute to domoic acid indirect photolysis is singlet oxygen ($^1O_2$). Loss of $^1O_2$ is dominated by deactivation by water. To extend $^1O_2$ lifetimes, 90% of the water in the synthetic matrices was replaced with deuterium oxide (D_2O), resulting in [$^1O_2$] that was expected to be ~6.4 times higher than in the 100% H_2O matrix (2). In the seawater matrix, the observed domoic acid photodegradation rate constant increased from 25.4 (±1.0) × 10^{-6} s^{-1} in the 100% H_2O solution to 30.0 (±2.0) × 10^{-6} s^{-1} in the 90% D_2O/10% H_2O solution. This slight increase suggests that $^1O_2$ accounts for only 2.9% of indirect domoic acid photodegradation in seawater. Similarly low contributions of $^1O_2$ to domoic acid indirect photodegradation were determined for the freshwater matrix (4.1%) and the ionic strength matrix (9.5%), suggesting that $^1O_2$-mediated pathways are not dominant contributors to domoic acid photodegradation in any matrix.

Energy transfer (isomerization). As with other conjugated dienes (3, 4), energy transfer from ^{3}DOM* to domoic acid, a *cis-trans* isomer, formed three isomer products (5), confirmed by HPLC-MS analysis. Although the conformations of the isomer products were not determined, their concentrations were quantified by HPLC-UV at 242 nm because of similar molar extinction coefficients to domoic acid at this wavelength (5). Energy transfer reactions from triplet excited-state DOM (^{3}DOM*) were determined using the observed linear isomer formation for one of the product isomers (retention time, RT=17.8 min) in the first 6 hours in the presence of seawater halides or the first 10 hours in the freshwater and ionic strength control (Figure S1e). The total isomer formation rate was calculated by determining the ratios of the three isomer products to be 0.53:0.26:0.21 (with RT 17.8 min, 18.2 min, and 28.8 min respectively). The total isomerization rate was divided by the average domoic acid concentration over the timeframe to obtain the rate constant of isomerization (Figure S1f and Table S1).

The isomerization rate constant observed in the ionic strength control and the seawater halides solution were double the observed rate in the freshwater case, consistent with previously observed doubling of isomerization rates the presence of high ionic strength regardless of the identity of the salt (6). Furthermore, the observed increase in the isomerization rate constant could account for the observed increase in the indirect

photodegradation rate constant in the presence of ionic strength, but not the increase in the presence of seawater halides.

Electron transfer. Unlike $^1O_2$ and energy transfer reactions, which were estimated using pathway-specific techniques, electron transfer with ^{3}DOM* was evaluated by quenching the reaction using 25 mM phenol (7), which can also react with radicals (8). Phenol may also quench $^1O_2$; however, the contribution of $^1O_2$ to domoic acid photodegradation was found to be minor in earlier experiments using deuterium oxide. In order to test for additional scavenging of radical reactions, 25 mM methanol and, in the presence of halides, 250 mM isopropanol, were separately added to the synthetic solutions to quench radicals, as discussed below. The concentration of quenching agents (e.g. 25 mM phenol, 25 mM methanol, 250 mM isopropanol) was selected to maximize the quenching of the reactive intermediates under consideration. The effect of the addition of quencher Q on domoic acid (DA) degradation by intermediate I (where I is ^{3}DOM*, $^{\bullet}$OH, or RHS) was estimated using the ratio $k_{I,DA}[DA]/k_{I,Q}[Q]$, as reported in Table S5. The second-order rate constants ($k_{I,DA}$ for the reaction of the intermediate with domoic acid, $k_{Q,DA}$ for the reaction of the intermediate with the quenching agent) used in this calculation are presented in Table S4. When the value of this ratio is small (e.g. $\leq$0.05), the reaction of the intermediate I with domoic acid is expected to be quenched nearly completely. This criteria was met for all quenching conditions except for quenching some RHS ($Br^{\bullet}$, $Cl_2^{\bullet-}$, $Br_2^{\bullet-}$, $ClBr^{\bullet-}$) by 25 mM methanol (Table S5), discussed further in the next section.

The pseudo-first order rate constants of electron transfer reactions were calculated as the difference of the rate constant observed in the alcohol- and phenol-quenched matrixes under nearly complete quenching conditions. These electron transfer rate constants were determined to be 1.2 ($\pm$0.1)$\times$ 10^{-6} s^{-1} in freshwater (25 mM phenol and 25 mM methanol), 3.0 ($\pm$0.2)$\times$ 10^{-6} s^{-1} in the ionic strength control (25 mM phenol and 25 mM methanol) and 3.3 ($\pm$0.3)$\times$ 10^{-6} s^{-1} in the presence of seawater halides (25 mM phenol and 250 mM isopropanol).

Radicals. Radical-mediated reactions can be selectively scavenged using alcohols. Upon addition of 25 mM methanol, the observed first-order rate constant of domoic acid photodegradation decreased by 8% in freshwater and 1% in the ionic strength control. In the presence of seawater halides, the addition of 25 mM methanol resulted in a 27%

decrease, suggesting that radical-mediated reactions may have a greater contribution to domoic acid photodegradation in the presence of seawater halides. As indicated above, 25 mM methanol is expected to nearly completely quench $^{\bullet}$OH reactions with domoic acid. Because radicals anticipated to be prevalent in the presence of seawater halides (i.e. reactive halogen species, RHS) are less reactive with methanol than $^{\bullet}$OH, 250 mM isopropanol was added in separate experiments to quench these less reactive radical species (Table S5). In the presence of 250 mM isopropanol, which is expected to nearly completely quench RHS (Table S5), the observed first-order rate constant of domoic acid photodegradation in the presence of halides decreased by 55% from 25.4(±1.0) × 10^{-6} s^{-1} to 11.5 (±0.6) × 10^{-6} s^{-1}. This final value is similar to the observed first-order rate constant of domoic acid photodegradation in the ionic strength control (11.0 (±0.3) × 10^{-6} s^{-1}), suggesting that the increase in domoic acid photodegradation could be accounted for by radical reactions that can be scavenged by 250 mM isopropanol. As such, quenching experiments in natural water samples (Figure 1d) used identical quenching conditions to identify the contribution of this halide-driven radical-mediated pathway to domoic acid photodegradation in natural waters.

Reactions included in kinetic model. Kinetic modeling was performed as described previously (8, 9) using the computer program Kintecus 4.55 (10) (Section 1.5). Reactions modeled between organic chemicals and radical species were added to the model with rate constants described in Table S4 (7, 11-23).

Modeled initiation step for BrAP-sensitized reactions: The computational model (Fig. 2a) was performed using 2-bromoacetophenone (BrAP) as a sensitizer. The input of reactive species into the model was assumed to be completely attributable to the photolysis of BrAP to produce bromine radical (Br$^{\bullet}$). The rate constant of this reaction was calculated using the equation S1:

$$k_{Br\text{-}AP} = 2.303\ \Phi_\lambda\ I_\lambda\ \varepsilon_\lambda\ l \qquad [S1]$$

BrAP is known to produce Br$^{\bullet}$ with a quantum yield, Φ_λ = 0.4, upon irradiation with 300-350 nm light (24), and this quantum yield was assumed to be constant over all wavelengths. The photolysis rate of BrAP was calculated using wavelength-dependent photon flux, I_λ, from PNA/pyr actinometry. The molar extinction coefficient, ε_λ, was

determined using UV-Vis. Finally, the pathlength, *l,* in the quartz test tubes is 1.43 cm. Therefore, $Br^{\bullet}$ production from 100 μM BrAP was modeled to occur at 5.6×10^{-4} s^{-1}.

Oxidation of halides by synthetic aromatic ketone triplets. For synthetic aromatic ketone triplet sensitizers, the reduction potential of the triplet can be calculated from the sum of the standard reduction potential of the ground state sensitizer (SEN), $E°(SEN/SEN^{-})$, and its triplet energy, $E_T(SEN)$ (20). These calculations yielded 1.95 V_{NHE} for 3-benzoylpyridine, 1.83 V_{NHE} for benzophenone-4-carboxylate, 1.79 V_{NHE} for benzophenone, 1.63 V_{NHE} for acetophenone, and 1.34 V_{NHE} for 2-acetonaphthone. This triplet reduction potential, along with the reduction potential of the halide, X^{-}, ($E°(X/X^{-})$) (25), can be used to calculate the standard free energy of the charge transfer process (equations S2, S3).

$$^{3}SEN^{*} + X^{-} \rightarrow SEN^{\bullet-} + X^{\bullet} \qquad [S2]$$

$$\Delta G_{CT} = E°(X/X^{-}) - [E°(SEN/SEN^{-}) + E_T(SEN)] \qquad [S3]$$

The calculated ΔG_{CT} values can be used to determine the free energy of activation ($\Delta G^{\ddagger}$) for the formation of the charge-transfer exciplex (equation S4) using a derivation of the Marcus equation (equation S5), including the reorganization energy relating to the halides ($\overline{R}_{Cl^-} = 1.98$ eV, $\overline{R}_{Br^-} = 1.75$ eV) (25).

$$^{3}SEN^{*} + X^{-} \rightarrow {}^{3}(SEN^{-}\text{-}X) \qquad [S4]$$

$$\Delta G^{\ddagger} = (\overline{R}/4)(1 + \Delta G°_{CT}/\overline{R})^{2} \qquad [S5]$$

Using equation S7, the free energy of activation for the forward electron transfer was modeled as a function of triplet reduction potentials (Figure 3a). The change in the quantum yield of domoic acid photodegradation relative to the ionic strength control (540 mM $NaClO_4$) under different halide conditions was calculated from the observed first order rate constants of domoic acid photolysis (Table S1). The absorbance of the synthetic triplets (or SRDOM) was not affected by the presence of halides.

Estimation of radical concentrations. To obtain an estimate of total radical concentrations, $^{\bullet}OH$ steady-state concentrations ($[^{\bullet}OH]_{SS}$) were measured in synthetic freshwater and seawater halide samples using the method of Zhou and Mopper (26). In

freshwater, $[^{\bullet}OH]_{SS}$ was determined to be 8.3(±0.5) $\times 10^{-17}$ M. In seawater, $[^{\bullet}OH]_{SS}$ was found to be 1.1(±0.0) $\times 10^{-17}$ M.

Based on the measured $[^{\bullet}OH]_{SS}$ in seawater, estimates of RHS concentrations were made using the computational model described above. The model was developed to predict the concentrations of RHS in equilibrium with a constant steady-state concentration of $^{\bullet}OH$. To account for scavenging of radical oxidants by DOM, DOM was modeled by partitioning the total mass concentration of DOM (5 mg-C/L) into a more reactive component (i.e. hydroquinone, HQ) and a less reactive component (i.e. methanol), as previously validated (27). Because the exact ratio of these two components in DOM is unknown, the percent of DOM modeled as HQ was varied from 25-100%. In all cases, the concentration of radicals in solution was ~10^{-14} M, and most of these radicals (>99.9%) were RHS (Table S3). The concentration of RHS was three orders of magnitude higher than $[^{\bullet}OH]_{SS}$.

Modeled RHS concentrations are lower than those modeled in previous studies (28, 29) using anthroquinone-2-sulfonate (AQ2S) as a model triplet sensitizer (i.e., 10^{-13}-10^{-12} M $Br_2^{\bullet-}$ and 10^{-14}-10^{-12} M $Cl_2^{\bullet-}$). The higher concentrations measured in previous studies likely are due to the high reduction potential of AQ2S promoting direct oxidation of Cl^-; the AQ2S reduction potential is considered to be higher than that of natural organic matter (23).

Figures

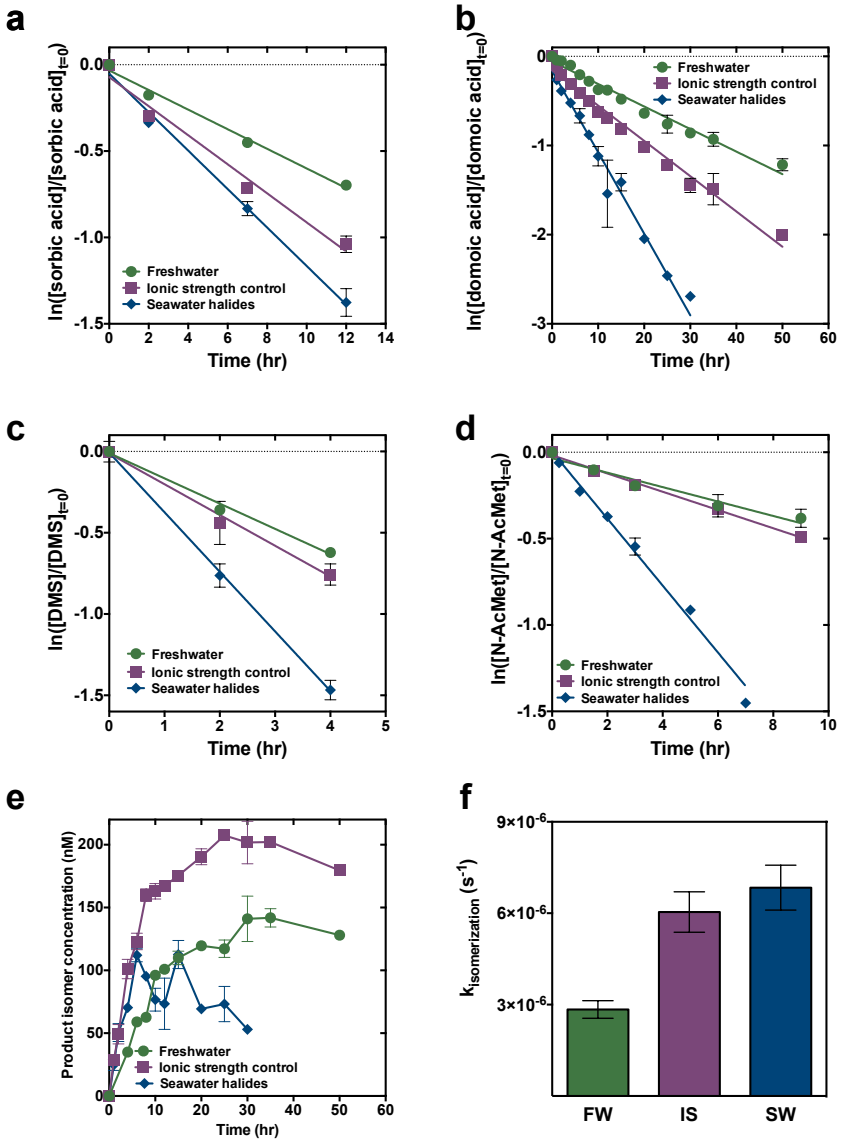

Figure S1: Photodegradation of target compounds in synthetic water matrices. Semi-log plots of sorbic acid (a), domoic acid (b), dimethyl sulfide (DMS) (c) and N-acetylmethionine (d) photodegradation in synthetic matrices containing contain 5 mg/L Suwannee River DOM at pH 8.1 with 20 mM phosphate buffer alone (freshwater), with 540 mM $NaClO_4$ (ionic strength control), or 540 mM NaCl and 0.8 mM NaBr (seawater halides). Initial concentration of all analytes was 2 µM. The slope of the lines represents the pseudo-first order rate constants presented in figure 1b. (e) Concentration of one domoic acid product isomer as a function of time. (f) Rate constant of isomerization during the first 10 hours of irradiation in the freshwater (FW) and ionic strength control (IS) matrices and 6 hours of irradiation in the seawater (SW) matrix. Error bars in (a-e) represent the standard error between duplicate experiments. Error bars in (f) represent the standard error of the slope obtained by linear regression of duplicate sets of semi-log transformed kinetic data.

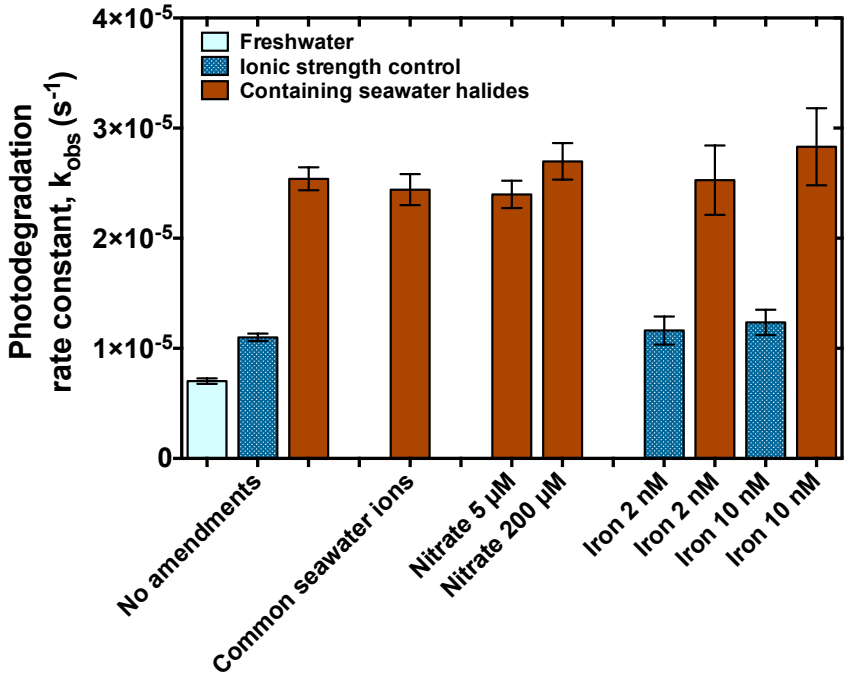

Figure S2: Effect of seawater constituents on domoic acid photodegradation in synthetic matrices. Samples without amendments are duplicated from Fig. 1b and contain 5 mg/L Suwannee River DOM at pH 8.1 with 20 mM phosphate buffer alone (freshwater), with 540 mM $NaClO_4$ (ionic strength control), or 540 mM NaCl and 0.8 mM NaBr (seawater halides). Common seawater ions contain 420 mM NaCl, 0.8 mM NaBr, 29 mM sodium sulfate (Na_2SO_4), 54 mM magnesium chloride ($MgCl_2•6H_2O$), 11 mM calcium chloride ($CaCl_2•2H_2O$), 10 mM potassium chloride (KCl), 0.35 mM boric acid (H_3BO_3), 1.8 mM sodium bicarbonate ($NaHCO_3$) and 0.26 mM sodium carbonate (Na_2CO_3). Nitrate or iron-amended samples contain the nitrate and iron concentrations indicated. Error bars represent the standard error of the slope obtained by linear regression of duplicate sets of semi-log transformed kinetic data.

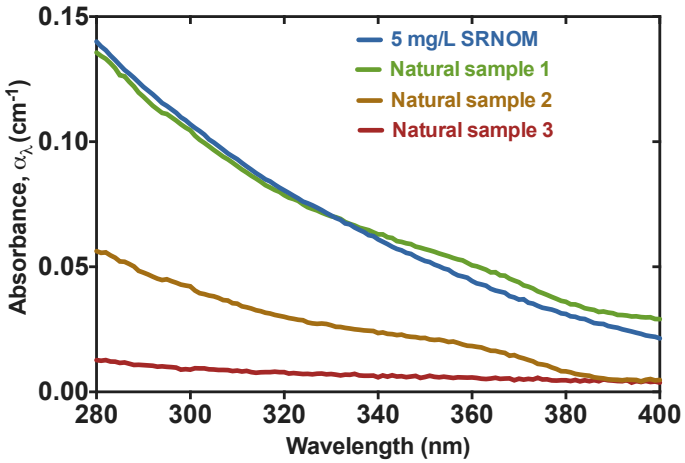

Figure S3: Absorbance spectra of natural water samples.

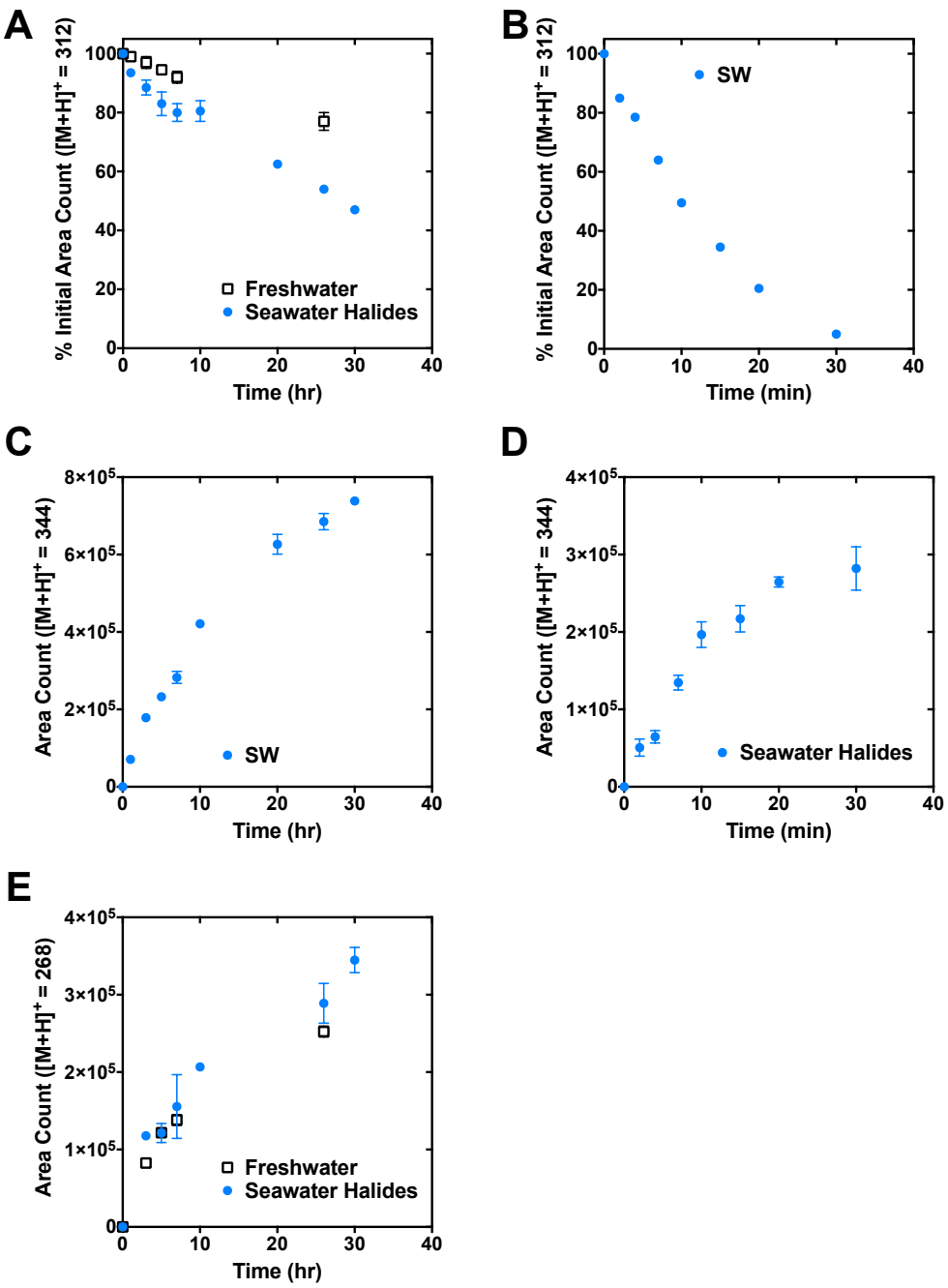

Figure S4: Ions detected in positive scan mode using LC-MS. The percentage of the initial area counts for ions with $[M+H]^+ = 312$ (domoic acids and its isomers) during photodegradation sensitized by 12.5 mg/L SRNOM (A) and 250 µM BrAP (B) in a freshwater matrix or in the presence of seawater halides. Area counts for ion $[M+H]^+ = 344$ sensitized by 12.5 mg/L SRNOM (C) and 250 µM BrAP (D) in the presence of seawater halides. The ion ($[M+H]^+ = 344$) was not identified in the synthetic freshwater matrix containing SRNOM as a sensitizer. Area counts for ion $[M+H]^+ = 268$ sensitized by 12.5 mg/L SRNOM (E) in a synthetic freshwater matrix or in the presence of seawater halides. The ion ($[M+H]^+ = 268$) was not identified in the seawater halide matrix containing 250 µM BrAP as a sensitizer.

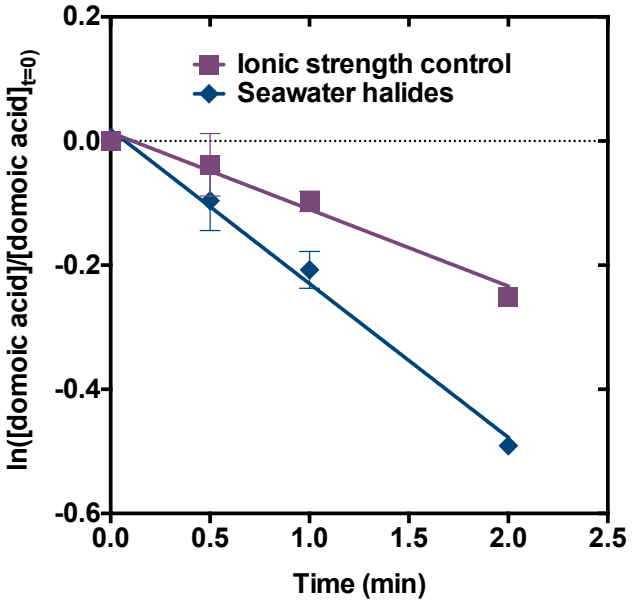

Figure S5: Domoic acid degradation initiated by gamma radiolysis. Solutions contained 2 μM domoic acid, 5 mg/L Suwannee River NOM and 20 mM phosphate buffer (pH 8.1). In addition, the ionic strength control contained 540 mM $NaClO_4$, and seawater halides contained 540 mM NaCl and 0.8 mM NaBr.

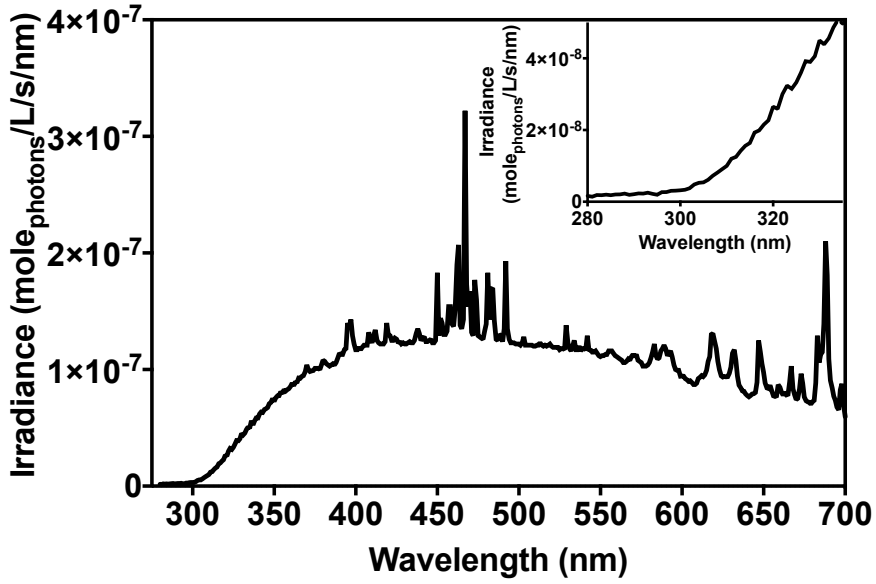

Figure S6: Lamp spectrum for photochemical experiments.

Tables

Table S1: Observed rate constants used to evaluate the contribution of pathways to domoic acid photodegradation in synthetic solutions.

Condition	Freshwater	Ionic strength control	Seawater halides
Direct photolysis			
2 μM	1.8 (±0.2)× 10^{-6}	2.6 (±0.2)× 10^{-6}	4.0 (±0.5)× 10^{-6}
2 μM w/SRDOM shading[a]	1.6 (±0.2)× 10^{-6}	2.3 (±0.2)× 10^{-6}	3.6 (±0.5)× 10^{-6}
Indirect photodegradation			
5 mg/L SRNOM	7.0 (±0.2)× 10^{-6}	11.0 (±0.3)× 10^{-6}	25.4 (±1.0)× 10^{-6}
90% D_2O/10%H_2O	8.8 (±0.6)× 10^{-6}	17.6 (±1.0)× 10^{-6}	30.0 (±2.0)× 10^{-6}
Isomerization rate	2.8 (±0.3)× 10^{-6}	6.0 (±0.7)× 10^{-6}	6.8 (±0.7)× 10^{-6}
25 mM phenol	5.2 (±0.4)× 10^{-6}	7.9 (±0.4)× 10^{-6}	8.2 (±0.7)× 10^{-6}
25 mM methanol	6.4 (±0.1)× 10^{-6}	10.9 (±0.5)× 10^{-6}	18.5 (±2.0)× 10^{-6}
250 mM isopropanol	N.M[b]	N.M[b]	11.5 (±0.6)× 10^{-6}

[a] Values calculated using solution absorbance.

[b] N.M. = Not measured.

Table S2: Measured water quality parameters of natural water samples.

	[Cl^-], mM	[Br^-], mM	[NO_3^-], μM	[Fe], nM[a]	pH	TOC (mg-C/L)
Natural sample 1 San Francisco Bay	400	0.6	175	ND	7.9	6.0
Natural sample 2 San Francisco Bay	495	0.7	5	ND	7.9	2.6
Natural sample 3 Monterey Bay	546	0.9	3	ND	8.2	1.3

[a] Detection limit was 20 nM.

Table S3: Modeled RHS concentrations in equilibrium with measured [$^{\bullet}$OH]$_{SS}$ = 1.1 ×10^{-17} M in synthetic seawater. DOM mass concentration (5 mg-C/L) is modeled as hydroquinone (HQ; percent indicated), and methanol (the remaining percentage).

% HQ	[Cl$^{\bullet}$]$_{SS}$, M	[Br$^{\bullet}$]$_{SS}$, M	[Cl$_2^{\bullet-}$]$_{SS}$, M	[ClBr$^{\bullet-}$]$_{SS}$, M	[Br$_2^{\bullet-}$]$_{SS}$, M	Total RHS, M	Ratio of Total RHS to [$^{\bullet}$OH]$_{SS}$
25	5.1×10^{-21}	2.1×10^{-17}	7.2×10^{-18}	1.2×10^{-14}	3.2×10^{-14}	**4.4×10^{-14}**	**3998**
40	3.2×10^{-21}	1.3×10^{-17}	4.5×10^{-18}	7.4×10^{-15}	2.0×10^{-14}	**2.8×10^{-14}**	**2509**
50	2.6×10^{-21}	1.1×10^{-17}	3.6×10^{-18}	5.9×10^{-15}	1.6×10^{-14}	**2.2×10^{-14}**	**2010**
60	2.2×10^{-21}	8.8×10^{-18}	3.0×10^{-18}	4.9×10^{-15}	1.4×10^{-14}	**1.8×10^{-14}**	**1677**
75	1.7×10^{-21}	7.1×10^{-18}	2.4×10^{-18}	4.0×10^{-15}	1.1×10^{-14}	**1.5×10^{-14}**	**1343**
95	1.4×10^{-21}	5.6×10^{-18}	1.9×10^{-18}	3.1×10^{-15}	8.5×10^{-15}	**1.2×10^{-14}**	**1061**
100	1.3×10^{-21}	5.3×10^{-18}	1.8×10^{-18}	3.0×10^{-15}	8.1×10^{-15}	**1.1×10^{-14}**	**1008**
60[a]	7.9×10^{-21}	1.7×10^{-17}	1.1×10^{-17}	1.8×10^{-14}	7.1×10^{-17}	**1.8×10^{-14}**	**1650**

[a] Modeling was performed excluding the pathway ($ClBr^{\bullet-} + Br^- \rightarrow Br_2^{\bullet-} + Cl^-$) to demonstrate the significance of this pathway to form $Br_2^{\bullet-}$ from $ClBr^{\bullet-}$, which is expected to be the primary RHS formed initially via halide oxidation by ^{3}DOM* (equation 3 in manuscript).

Table S4: Second order rate constants (M^{-1} s^{-1}) for reactions of photoproduced reactive intermediates with organic compounds.

Reactive Intermediate: / Organic Substrate:	$^{\bullet}OH$	$Cl^{\bullet}$	$Br^{\bullet}$	$Cl_2^{\bullet-}$	$Br_2^{\bullet-}$	$ClBr^{\bullet-}$	$^3DOM^*$
Domoic acid	9.2×10^9 (a)	1.5×10^9 (d)	3.3×10^9 (i)	6.8×10^8 (l)	6.8×10^8 (n)	6.8×10^8 (n)	5.6×10^9 (r)
***tert*-Butanol**	5.2×10^8 (b)	1.5×10^9 (e)	1.4×10^4 (j)	7.0×10^2 (m)	7.0×10^2 (n)	7.0×10^2 (n)	N.A. (s)
Methanol	9.0×10^8 (b)	5.7×10^9 (f)	3.0×10^5 (j)	3.5×10^3 (m)	4.4×10^3 (o)	4.4×10^3 (q)	N.A. (s)
Isopropanol	2.2×10^9 (b)	3.7×10^9 (g)	6.6×10^6 (j)	1.2×10^5 (m)	1.2×10^5 (n)	1.2×10^5 (n)	N.A. (s)
Phenol	1.4×10^{10} (c)	2.5×10^{10} (h)	6.2×10^9 (k)	2.5×10^8 (m)	6.1×10^6 (p)	6.1×10^6 (q)	1.8×10^9 (t)

(a) Value from Jones et al. (12).
(b) Value from Willson et al. (13).
(c) Value from Land and Ebert (14).
(d) Value from Gilbert et al. (15) for reaction with fumaric acid.
(e) Value from Gilbert et al. (15).
(f) Value from Chateauneuf (16).
(g) Value from Sumiyoshi et al. (17).
(h) Value from Alfassi et al. (18).
(i) Value from Guha et al. (19) for reaction with linolenic acid.
(j) Value from Merényi and Lind (20).
(k) Value from Merényi and Lind for reaction with 4-iodophenol (20).
(l) Value from Hasegawa and Neta (11) for reaction with sorbic acid.
(m) Value from Hasegawa and Neta (11).
(n) Value estimated from rate constant with $Cl_2^{\bullet-}$.
(o) Value from Fel'dman et al. (21).
(p) Value from Alfassi et al. (22).
(q) Value estimated from rate constant with $Br_2^{\bullet-}$.
(r) Value selected is the upper bound of rate constants for oxidation by triplets reported in Canonica et al. (23).
(s) N.A. = Not applicable. Aliphatic alcohols are not expected to significantly quench $^3DOM^*$.
(t) Value from Halladja et al. (7) for reaction with 2,4,6-trimethylphenol.

Table S5: Calculated effect of quencher (Q) addition on domoic acid photodegradation (DA) by individual photoproduced reactive intermediates (I). Values significantly lower than 1 (e.g. ≤0.05) suggest nearly complete quenching. Values in bold do not meet this criteria.

$k_{I,DA}[DA]/k_{I,Q}[Q]$	**$^{\bullet}$OH**	**$Cl^{\bullet}$**	**$Br^{\bullet}$**	**$Cl_2^{\bullet-}$**	**$Br_2^{\bullet-}$**	**$ClBr^{\bullet-}$**	**^{3}DOM***
25 mM phenol	5×10^{-5}	5×10^{-6}	4×10^{-5}	2×10^{-4}	9×10^{-3}	9×10^{-3}	2×10^{-4}
25 mM methanol	8×10^{-4}	2×10^{-5}	**9×10^{-1}**	**2×10^{1}**	**1×10^{1}**	**1×10^{1}**	N.A.[(a)]
250 mM isopropanol	3×10^{-5}	3×10^{-6}	4×10^{-3}	5×10^{-2}	5×10^{-2}	5×10^{-2}	N.A.[(a)]

[(a)] N.A. = Not applicable. Aliphatic alcohols are not expected to significantly quench ^{3}DOM*.

Supplementary References

1. Leifer A (1988) *The Kinetics of Environmental Aquatic Photochemistry: Theory and Practice* (American Chemical Society, Washington, D.C.).

2. Cory RM, Cotner JB, McNeill K (2009) Quantifying interactions between singlet oxygen and aquatic fulvic acids. *Environ Sci Technol* 43(3):718–723.

3. Zepp RG, Schlotzhauer PF, Sink RM (1985) Photosensitized transformations involving electronic energy transfer in natural waters: Role of humic substances. *Environ Sci Technol* 19(1):74–81.

4. Grebel JE, Pignatello JJ, Mitch WA (2011) Sorbic acid as a quantitative probe for the formation, scavenging and steady-state concentrations of the triplet-excited state of organic compounds. *Water Res* 45(19):6535–6544.

5. Bouillon R-C, Kieber RJ, Skrabal SA, Wright JL (2008) Photochemistry and identification of photodegradation products of the marine toxin domoic acid. *Mar Chem* 110(1-2):18–27.

6. Parker KM, Pignatello JJ, Mitch WA (2013) Influence of Ionic Strength on Triplet-State Natural Organic Matter Loss by Energy Transfer and Electron Transfer Pathways. *Environ Sci Technol* 47(19):10987–10994.

7. Halladja S, Halle Ter A, Aguer J-P, Boulkamh A, Richard C (2007) Inhibition of humic substances mediated photooxygenation of furfuryl alcohol by 2,4,6-trimethylphenol. Evidence for reactivity of the phenol with humic triplet excited states. *Environ Sci Technol* 41(17):6066–6073.

8. Grebel JE, Pignatello JJ, Mitch WA (2010) Effect of halide ions and carbonates on organic contaminant degradation by hydroxyl radical-based advanced oxidation processes in saline waters. *Environ Sci Technol* 44(17):6822–6828.

9. Yang Y, Pignatello JJ, Ma J, Mitch WA (2014) Comparison of Halide Impacts on the Efficiency of Contaminant Degradation by Sulfate and Hydroxyl Radical-Based Advanced Oxidation Processes (AOPs). *Environ Sci Technol* 48(4):2344–2351.

10. Ianni JC (2012) *Kintecus, Windows Version 4.55* Available at: http://www.kintecus.com.

11. Hasegawa K, Neta P (1978) Rate constants and mechanisms of reaction of Cl_2^- radicals. *J Phys Chem* 82(8):854–857.

12. Jones KG, Cooper WJ, Mezyk SP (2009) Bimolecular Rate Constant Determination for the Reaction of Hydroxyl Radicals with Domoic and Kainic Acid in Aqueous Solution. *Environ Sci Technol* 43(17):6764–6768.

13. Willson RL, Greenstock CL, Adams GE, Wageman R, Dorfman LM (1971) The standardization of hydroxyl radical rate data from radiation chemistry. *Int J Rad Phys Chem* 3(3):211–220.

14. Land EJ, Ebert M (1967) Pulse Radiolysis Studies of Aqueous Phenol. Water Elimination from Dihydroxycyclohexadienyl Radicals to form Phenoxyl. *Trans Faraday Soc* 63:1181-1190.

15. Gilbert BC, Stell JK, Peet WJ, Radford KJ (1988) Generation and reactions of the chlorine atom in aqueous solution. *J Chem Soc, Faraday Trans 1* 84(10):3319-3330.

16. Chateauneuf JE (1990) Direct measurement of the absolute kinetics of chlorine atom in carbon tetrachloride. *J Am Chem Soc* 112(1):442–444.

17. Sumiyoshi T, Miura K, Hagiwara H, Katayama M (1987) On the Reactivity of Chlorine Atoms towards Alcohols. *Chem Lett* 7:1429-1430.

18. Alfassi ZB, Mosseri S, Neta P (1989) Reactivities of Chlorine Atoms and Peroxyl Radicals Formed in the Radiolysis of Dichloromethane. *J Phys Chem* 93(4):1380-1385.

19. Guha SN, Schöneich C, Asmus KD (1993) Free radical reductive degradation of vic-dibromoalkanes and reaction of bromine atoms with polyunsaturated fatty acids: Possible involvement of $Br^{\bullet}$ in the 1,2-dibromoethane-induced lipid peroxidation. *Arch Biochem Biophys* 305(1):132–140.

20. Merényi G, Lind J (1994) Reaction Mechanism of Hydrogen Abstraction by the Bromine Atom in Water. *J Am Chem Soc* 116(17):7872–7876.

21. Fel'dman VI, Belevskii VN, Bugaenko LT, Moralev VM, Popov VI (1986) Early ionic processes in the radiolysis of liquid methanol. *High Energy Chem* 20:2.

22. Alfassi ZB, Huie RE, Neta P, Shoute LCT (1990) Temperature Dependence of the Rate Constants for Reactions of Inorganic Radicals with Organic Reductants. *J Phys Chem* 94(25):8800-8805.

23. Canonica S, Hellrung B, Wirz J (2000) Oxidation of phenols by triplet aromatic ketones in aqueous solution. *J Phys Chem A* 104(6):1226–1232.

24. McGimpsey WG, Scaiano JC (1988) Photochemistry of α-chloro- and α-bromoacetophenone. Determination of extinction coefficients for halogen–benzene complexes. *Can J Chem* 66(6):1474–1478.

25. Loeff I, Rabani J, Treinin A, Linschitz H (1993) Charge Transfer and Reactivity of $n\pi^*$ and $\pi\pi^*$ Organic Triplets, Including Anthraquinonesulfonates, in Interactions with Inorganic Anions: A Comparative Study Based on Classical Marcus Theory. *J Am Chem Soc* 115(20):8933–8942.

26. Zhou X, Mopper K (1990) Determination of photochemically produced hydroxyl radicals in seawater and freshwater. *Mar Chem* 30:71–88.

27. Grebel JE, Pignatello JJ, Song W, Cooper WJ, Mitch WA (2009) Impact of halides on the photobleaching of dissolved organic matter. *Mar Chem* 115(1-2):134–144.

28. De Laurentiis E, et al. (2012) Assessing the occurrence of the dibromide radical ($Br_2^{\bullet-}$) in natural waters: Measures of triplet-sensitised formation, reactivity, and modelling. *Sci Total Environ* 439:299–306.

29. Brigante M, et al. (2014) Formation and reactivity of the dichloride radical ($Cl_2^{\bullet-}$) in surface waters: A modelling approach. *Chemosphere* 95:464–469.